Wrexham University Research Online

Conference Paper

Electronic Stabilisation of Motorcycle Headlight Beams Using IMU-Based Orientation Sensing

Weinfurtner, E., Knox, D., and Jones, M.

This is a paper presented at the 10th International Conference on Mechatronics Engineering (ICOM'26), IEEE, Malaysia, Online.

Copyright of the author(s). Reproduced here with their permission and the permission of the conference organisers.

This accepted manuscript is licensed under a Creative Commons Attribution 4.0 International (CC BY 4.0) licence: https://creativecommons.org/licenses/by/4.0/.

Recommended citation:

Weinfurtner, E., Knox, D. and Jones, M. (2026) 'Electronic stabilisation of motorcycle headlight beams using IMU-based orientation sensing', in *2026 10th International Conference on Mechatronics Engineering (ICOM)*, Kuala Lumpur, Malaysia, 8–9 September. IEEE, pp. 1–7. doi: 10.1109/ICOM71159.2026.11726236.

Electronic Stabilisation of Motorcycle Headlight Beams Using IMU-Based Orientation Sensing

Elia Weinfurtner
Wrexham University
Wrexham, UK

Daniel Knox
Wrexham University
Wrexham, UK

Martyn Jones
Wrexham University
Wrexham, UK

2026 10th International Conference on Mechatronics Engineering (ICOM) | 979-8-3195-0952-9/26/$31.00 ©2026 IEEE | DOI: 10.1109/ICOM71159.2026.11726236

***Abstract*—A motorcycle headlight beam loses its correct direction during braking, acceleration, and cornering, since pitch and roll motion are not compensated by a fixed headlight. Existing adaptive front-lighting systems solve this using mechanical actuators, which add cost and can wear out over time. This paper presents a low-cost, solid-state alternative: a laboratory proof-of-concept that measures motorcycle orientation using an inertial measurement unit and converts roll and pitch into a symbolic beam response shown on individually controllable LED rings. Three orientation estimation methods were implemented and compared, and a Complementary filter was selected as the practical default. Static tests showed close agreement between applied and measured angles across $\pm 30^{\circ}$, dynamic roll tracking remained stable, while dynamic pitch tracking was more sensitive to motion. These results show that the proposed solid-state approach is technically feasible for adaptive beam stabilisation.**

***Index Terms*—adaptive headlight, motorcycle safety, inertial measurement unit, solid-state lighting, beam stabilisation**

I. Introduction

Night riding on a motorcycle is more difficult than night driving in a car. The headlight is almost the rider's only source of visual information about the road ahead. On a dark country road, hazards such as potholes or animals can only be seen once the headlight beam reaches them [1], [2].

A motorcycle also moves differently than a car. Cars remain level on the road, but a motorcycle leans, pitches, and rolls during normal riding. When the rider brakes or accelerates, the bike pitches forward or backward, and the beam moves down or up with it. When the rider corners, the bike rolls, and the beam rotates with it [3], [4]. As a result, the low-beam cut-off line no longer points on the road in the way it should for safe night riding [5], [6].

Adaptive front-lighting systems were created to solve this problem. However, most existing systems use mechanical parts, such as motors and mirrors, to move the headlight, and these systems are often found only on expensive high-end motorcycles [5], [7]. For example, the BMW adaptive headlight uses a xenon projector with a mirror that is moved by a servo motor to compensate for the lean angle [8]. This method works, but moving mechanical parts can wear out or fail over time.

This paper proposes a simpler and cheaper solid-state alternative that eliminates the need for moving parts. The proposed system measures the motorcycle's orientation in real time and uses these data to control the light pattern shown by NeoPixel LED rings, instead of physically moving the headlight [6], [7]. The main contribution of this paper is a laboratory-based proof-of-concept that demonstrates, builds, and evaluates this electronic beam-stabilisation approach, showing whether the underlying control principle can work before any road-legal or optically realistic version is considered. The reported results describe the beam-stabilisation principle only and do not represent measured road-safety outcomes.

II. Related Work

A. Motorcycle Dynamics and Night-Time Visibility

A motorcycle does not remain upright on its own and requires continuous input from the rider, unlike a car [3], [9], [10]. Its motion is usually modelled using coupled degrees of freedom, including roll, pitch, yaw, and steering angle [3], [9]. Roll is closely related to cornering, as the lean angle, steering angle, and tyre forces change together as the turning radius decreases [11], [12]. Pitch is mainly associated with braking and acceleration, as hard braking transfers weight to the front wheel and can lift the rear wheel if the deceleration is too high [4]. Roll and pitch are therefore the two motions most responsible for changes in the direction of the headlight beam during riding [3], [4], [9], [12].

A motorcycle is also harder for other drivers to see at night than a larger vehicle, as lights become the main visual signal [1], [13], which can cause drivers to misjudge the distance or speed of an approaching motorcycle [1], [13].

Beam quality affects what the rider can see. Measurements of nine motorcycle headlights showed large differences in low- and high-beam range, and poor aiming was found to reduce road illumination or increase glare [15]. Fig. 1 compares a standard low-beam pattern with an adaptive one, showing a more uniform light distribution. Glare can cause temporary loss of vision, with two-wheeler riders particularly affected [16], [17].

B. Evolution of Adaptive Front-Lighting Systems

Adaptive front-lighting systems (AFS) were developed to overcome the limitation of fixed headlights and later benefited from LED technology, which improved both efficiency and flexibility [2], [5], [18]. Early systems used xenon sources with mechanical actuators, while later designs evolved towards individually controllable LED and matrix-based sources to enable more flexible beam shaping [18]. Modern architectures integrate sensing, control, and actuator layers and can support different lighting modes under varying driving conditions [19]. Camera-based systems can measure vehicle pitch in real time and adjust the beam angle without requiring a dedicated angle sensor [20], while inertial sensing can keep the beam closer to its optimal angle than suspension levelling alone [21].

TABLE I
MICROCONTROLLER PLATFORM COMPARISON

Platform	Clock Speed	Flash/RAM	Digital I/O	Interfaces	Approx. Cost	Main Limitation
GIGA R1 WiFi	480/240 MHz	2 MB/1 MB	76	3×I²C, 2×SPI, 4×UART	£67	—
Mega 2560	16 MHz	256 KB/8 KB	54	1×I²C, 1×SPI, 4×UART	£45	Too limited for simultaneous IMU, LED, and display use
ESP32 DevKitC V4	240 MHz	4 MB/520 KB	34	2×I²C, 2×SPI, 2×UART	£8	Less headroom; some GPIO pins constrained by flash/PSRAM
Teensy 4.1	600 MHz	7.9 MB/1024 KB	55	3×I²C, 3×SPI, 8×UART	£24	Less directly integrated with the chosen display/sensor platform

Motorcycle-specific systems remain less developed. Some prototypes use a gyroscope and a microcontroller to adjust the beam during cornering [6], while others adjust the intensity of the high-beam with vehicle speed to limit glare in slow traffic [7], or use an ultrasonic sensor and light-dependent resistors to control the output of left and right LED independently [23]. These studies indicate a shift from mechanically based automotive systems towards sensor-driven, electronically controlled solutions [6], [7], [23]. A recent review of adaptive headlight beam control confirms this same shift from mechanical actuation toward electronic, sensor-driven approaches [22].

III. SYSTEM DESIGN AND METHODOLOGY

A. MEMS IMU Sensing and Real-Time Filtering

An inertial measurement unit (IMU) combines an accelerometer and a gyroscope, enabling simultaneous measurement of inclination and angular rate [24]–[26]. Micro-electro-mechanical system (MEMS) sensors are well suited to embedded applications because they are small, low-power, and low-cost [25], [27]; however, consumer-grade devices can suffer from scaling errors, axis misalignment, and bias drift that persist even after calibration [26], [27]. For motorcycles, direct and reliable measurement of roll angle is difficult, so practical systems usually estimate it indirectly from sensor data and a mathematical model [28]. Reliable orientation estimation, therefore, requires sensor fusion: gyroscope-based estimates drift over time, whereas accelerometer-based estimates are more stable but noisier [29], [30]. The Complementary filter combines a low-pass accelerometer path with a high-pass gyroscope path to reduce both drift and noise, and its low computational cost makes it suitable for embedded systems [30], [31]. More advanced filters, such as Kalman and Madgwick, can offer higher accuracy at the expense of increased computational cost [30], [32].

On the output side, individually controllable LEDs such as the WS2812B are driven through a single serial data line, but the physical LED order must be correctly mapped in software to produce the intended pattern [33]. The reviewed literature confirms that roll and pitch are the motions most relevant to beam stability, that low-cost MEMS IMUs are practical yet imperfect, and that the Complementary filter offers a reasonable balance between simplicity and stability for an LED-based demonstrator.



Fig. 1. Comparison of standard and adaptive low-beam resolution [14].

B. Development Strategy and Requirements

This project was developed as a proof-of-concept prototype, not a road-ready motorcycle headlight system. The LED rings produce a symbolic light pattern that represents the beam response; the LED rings do not reproduce a certified optical headlamp beam, so these results do not show real-world road-safety performance. The aim was to show that adaptive control works in a realistic, low-cost laboratory setting, since production-grade optics, vehicle integration, and road validation would have exceeded available time and budget [5], [7]. Mechanical actuation was not included and testing was conducted under laboratory conditions to avoid the safety, legal, and logistical problems associated with road trials.

The development followed an iterative strategy consisting of concept definition, simplified prototype development, functional verification, embedded integration, and refinement. The process progressed from basic feasibility (whether pitch and roll motion could be measured and translated into a visible beam response) to improved response quality, visual stability, and robustness.

The prototype had to detect roll and pitch, the two motions most directly linked to cornering and longitudinal load transfer [4], [12], and convert these readings into a symbolic beam response, operating in real time without becoming visually unstable [29], [31]. It also had to remain low-cost, solid-state, and suitable for embedded implementation [5]–[7]; camera-based glare avoidance and light-sensing automation were deliberately excluded as beyond the project scope. The requirements were therefore defined around four expectations: orientation detection, visible symbolic beam adaptation, stable real-time behaviour, and simple, low-cost demonstrator operation.

C. Design Process and Validation Criteria

The design moved away from an initial cornering-light concept after it became clear that changes in motorcycle attitude can alter the direction of the entire low beam, not just the corner-entry region. A real motorcycle headlight was not practical because of cost, regulatory, and integration challenges, so the design shifted towards a symbolic beam

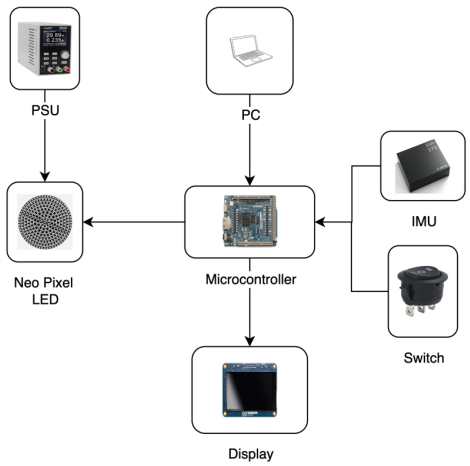


Fig. 2. Hardware architecture of the prototype.

demonstrator focused on the control principle rather than full optical compliance. The key step involved a virtual matrix model superimposed on the physically circular LED rings, allowing roll to be represented as a rotation and pitch as a vertical shift of the beam pattern, instead of a basic on/off ring response.

The prototype was evaluated against five criteria: a visible response to both roll and pitch, a stable beam at rest, beam movement in the correct direction, and reproducible behaviour, together with four practical criteria covering reaction speed, stability, robustness, and beam clarity. A successful outcome required a stable symbolic cut-off after calibration, a logical response to motion, and only a small visible delay; road-legal light output, certified glare control, and full safety validation were beyond the intended scope.

D. Hardware Architecture and Component Selection

The hardware was organised as a compact embedded system comprising sensing, processing, output, and user-interaction blocks, as shown in Fig. 2. The Arduino GIGA R1 served as the main processing unit, motion input was provided by an inertial measurement unit (IMU), and visible light output was generated by NeoPixel LED rings, with a GIGA Display Shield used for local visual feedback and a switch for beam-mode selection. Two separate power connections were employed: one for the LED rings and one for the microcontroller. A connected PC provided code upload, serial communication, and calibration support.

The IMU formed the sensing stage, the Arduino GIGA R1 the processing stage, and the LED rings the visual actuation stage. Although the IMU is physically mounted on the display shield, it was treated as a separate functional block because its sensing role differs from the display's monitoring function. This distinction provides the prototype with a clear hardware hierarchy consisting of sensor input, embedded processing, light output, and supporting user-interface hardware.

Components were selected to provide a balanced solution for a low-cost proof of concept rather than to closely match a production headlight. The Arduino GIGA R1 WiFi was chosen for its combination of processing power, memory, and interface flexibility, offering a dual-core processor running at up to 480/240 MHz, 2 MB of Flash, 1 MB of RAM, and three I2C, two SPI, and four UART interfaces, as summarised in Table I. By comparison, the Mega 2560 (16 MHz, 54 digital I/Os, four UARTs) was too limited for simultaneous IMU, LED, and display use; the ESP32 (up to 240 MHz, 520 kB SRAM) provided less headroom and had more constrained GPIO resources; and the Teensy 4.1 (600 MHz, 1024 kB RAM, 55 digital I/Os) was powerful but less compatible with the chosen display and sensor platform. The GIGA Display Shield, which integrates a BMI270 IMU, combines a display and a 6-axis sensor in a single unit. WS2812B-based LED rings were selected for beam output because they operate at 5 V and were available in a ring configuration that matches the intended circular beam geometry.

Fig. 3 shows the front view of the completed prototype, built from these components.

IV. Orientation Estimation and Control Algorithm

A. Sensor Data Acquisition

The BMI270 inertial measurement unit (IMU), mounted on the GIGA Display Shield, was accessed through the secondary I2C interface using the BoschSensorClass library. IMU servicing was performed using a timed routine rather than a blocking loop, so the update interval was derived from the actual elapsed time and used consistently in the calculations, instead of relying on approximate delays.

A key preprocessing step involved converting the raw sensor readings from the sensor frame into the prototype frame. This required a 90° rotation about the Y-axis, because the IMU is mounted at this angle inside the display shield. The prototype axes were defined as X for up-down motion, Y for right-left motion, and Z for forward motion, as shown in Fig. 4. Keeping this mapping explicit in the code, rather than embedding it within the angle calculations, made it easier to trace any subsequent filter behaviour back to a simple axis-definition error if necessary.

Before any filtering took place, the gyroscope bias was calibrated. A dedicated routine sampled the gyroscope while the prototype was held stationary, averaged the readings, and stored the result as an offset to be subtracted during later use. Without this step, even a small constant offset would

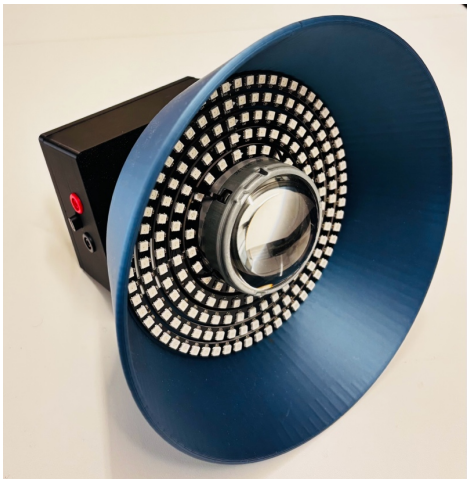


Fig. 3. Front view of the final prototype.

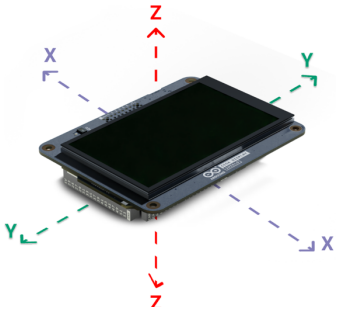


Fig. 4. IMU orientation diagram showing the defined prototype axes.

accumulate through integration and gradually distort the roll and pitch estimates.

B. Orientation Estimation Modes

Converting noisy IMU data into a beam response that appears stable and convincing on a low-resolution LED display was the main software challenge in this project. To resolve this issue, three orientation estimation modes were implemented and compared: accelerometer-only, Complementary filter, and Madgwick filter.

The accelerometer-only mode calculated roll and pitch directly from the accelerometer readings using the `atan2` function. This mode was not intended as the final output; instead, it served as a baseline estimate, a correction reference for the Complementary filter, and a simple comparison mode during development. It also allowed axis directions and static behaviour to be verified before more advanced fusion methods were applied.

The Complementary filter, shown in Fig. 5, became the practical default for the prototype because it provided the best balance between response speed, stability, and ease of tuning. The filter first calculates an accelerometer trust value, then derives separate weighting factors for roll and pitch, integrates the gyroscope readings, and finally fuses the result with the accelerometer angle. Fast motion is therefore captured by the gyroscope term, whereas long-term correction is provided by the accelerometer term. Roll and pitch are not treated identically: roll is allowed to respond quickly, whereas pitch is damped more heavily because it was found to be more sensitive to linear acceleration during early testing. The filter update is given by

$$\theta_t = \alpha_{\text{eff}} \left(\theta_{t-1} + \omega \, \Delta t\right) + \left(1 - \alpha_{\text{eff}}\right) \theta_{\text{acc}} \qquad (1)$$

where θ_t is the filtered angle [deg] at the current time step, α_{eff} is the effective filter weighting [dimensionless] after adaptive accelerometer trust adjustment, θ_{t-1} is the filtered angle [deg] from the previous time step, ω is the angular rate [deg/s] from the gyroscope, Δt is the measured time interval

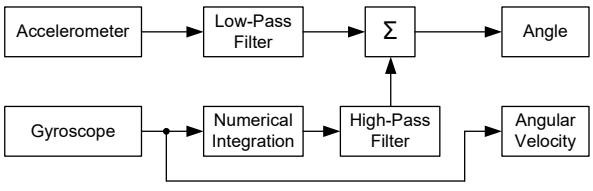


Fig. 5. Working principle of the Complementary filter.

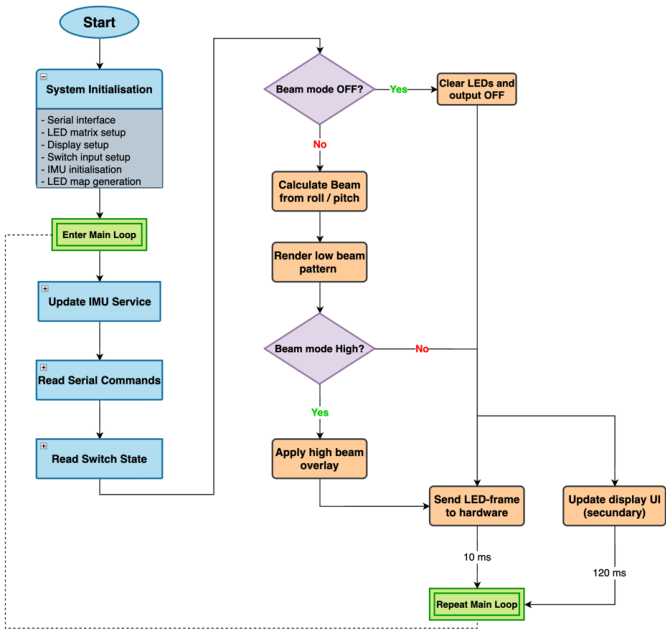


Fig. 6. Flow chart of the main program structure.

[s] between two filter updates, and θ_{acc} is the angle [deg] estimated directly from the accelerometer.

The Madgwick filter was also retained in the final software because it represents a technically relevant option that provides quaternion-based fusion [32]. In the implementation, the sensor data are first remapped into the internal reference frame, converted to radians, corrected using an adaptive beta factor, and passed to the quaternion update routine. However, this filter required more careful tuning in practice, and it tended to become either too slow or visually unstable depending on the selected beta value. It was retained in the code primarily to document the comparison process and to justify the final choice of the complementary filter.

C. Beam Mapping and Control Logic

The second part of the control logic converts the estimated orientation into a symbolic light pattern. Instead of treating the LED ring as a simple sequence of positions, each LED is assigned a virtual two-dimensional coordinate through a dedicated mapping routine. This approach enables the ring-shaped hardware to behave like a geometric rendering surface rather than a basic on/off light source.

Once this virtual map is established, roll is implemented as a rotation of the beam pattern, and pitch as a vertical shift of the cut-off line. In the rendering routine, each LED position is rotated, compared with the current cut-off position, and assigned a corresponding brightness value. The result is a simple mathematical beam model rather than a fixed on/off pattern.

A final processing stage was introduced between orientation estimation and LED output. The estimated roll and pitch values are first corrected using the chosen zero reference, then passed through a deadband, and finally smoothed separately before being sent to the LED strip. This step is important because a technically correct orientation estimate does not necessarily produce a visually clear command for a low-resolution LED display. Applying separate smoothing to roll

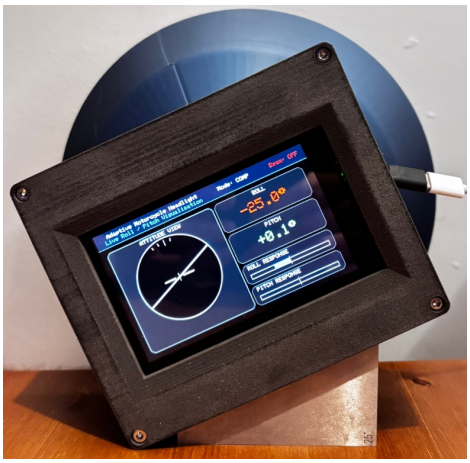


Fig. 7. Static roll test ($-25°$) display view.

and pitch improved the readability of the beam response and reduced visible jitter without altering the underlying estimation method.

Fig. 6 shows how these processing stages fit into the overall program structure. The software was implemented as a time-scheduled embedded loop because the prototype had to remain responsive when handling several tasks at different update rates. At startup, the system performs serial setup, LED initialisation, display setup, switch input configuration, IMU initialisation, and LED map generation, ensuring that the hardware reaches a known state before the main control loop begins. Inside the main loop, IMU servicing runs continuously, and serial commands remain available for tuning. The calibration and switch states are evaluated before any beam output is updated. The LED task executes at a defined interval rather than during every loop cycle, which reduces redundant updates and improves the determinism of the control path. The display is updated separately and at a lower rate than the beam-control path, ensuring that LED output timing is unaffected by the slower monitoring layer.

V. Testing and Results

A. Test Method

The prototype was tested under controlled indoor laboratory conditions using a structured test protocol. Before testing, the prototype was calibrated and reset to a reference position on a flat table surface via the serial interface, ensuring that all subsequent responses could be compared from the same starting point. Static roll and pitch angles were set using angle wedges and compared against both the on-screen display and the symbolic LED output on the front of the prototype. Fig. 7 illustrates the on-screen view of the prototype under the static roll test, whereas Fig. 8a shows the front view for the static pitch test.

Testing began with static roll and pitch, followed by combined static conditions and a static high-beam test, as shown in Fig. 8b, before proceeding to dynamic tests with slow and fast roll and pitch movements performed by hand. Stability and robustness were assessed at rest, under light touch, and under small vibration, followed by two functional tests covering the beam-mode switch and the low-beam brightness control. Finally, the three orientation estimation modes (accelerometer-only, Madgwick, and complementary filter) were compared under the same conditions, and selected tests were repeated three times to assess reproducibility. Reaction speed was measured using slow-motion video at 240 fps (corresponding to a frame interval of approximately 4.17 ms), analysed frame by frame to estimate the visible time lag between motion and beam response. Each test was scored on a scale of 1 to 5 against reaction speed, stability, robustness, and beam clarity.

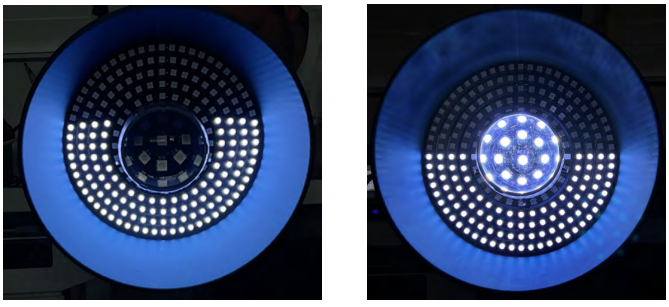
TABLE II
Experimental Results (Average Overall Score by Test)

Test ID	Score	Category
T1	5	Static Roll
T2	5	Static Pitch
T3	5	Static Combined
T4	4.75	Dynamic Roll (Slow)
T5	4.5	Dynamic Roll (Fast)
T6	3.25	Dynamic Pitch (Slow)
T7	3.25	Dynamic Pitch (Fast)
T8	5	Rest Stability Test
T9	4.25	Light Touch Disturbance
T10	5	Small Vibration Test
T11	5	Switch Test
T12	5	Low Beam Brightness
T13	2	Filter: ACC Only
T14	3.5	Filter: Madgwick
T15	4.5	Filter: Complementary
T16	5	Repeatability Test

B. Results

Table II summarises the average overall score achieved for each test. The static tests (T1–T3) all reached the maximum score of 5, confirming that the prototype reproduces the applied roll and pitch angles almost exactly, as illustrated in Fig. 7 and Fig. 8. The dynamic roll tests (T4, T5) also scored highly, while the dynamic pitch tests (T6, T7) scored noticeably lower, confirming that pitch is more sensitive to motion than roll.

The stability and robustness tests (T8–T10) and the functional tests (T11, T12) each achieved the maximum score, confirming reliable behaviour at rest and under minor disturbance. The repeatability test (T16) also reached the maximum score, showing that selected tests produced similar results across three repeated runs.



(a) (b)

Fig. 8. (a) Static pitch test ($-22.5°$) beam view; (b) Static high-beam test ($0°/0°$) beam view.

The filter comparison (T13–T15) gave the clearest technical result. The accelerometer-only mode scored only 2, since it reacted quickly but was highly sensitive to movement. The Madgwick filter scored 3.5, since it was stable but showed a significant delay. The Complementary filter scored highest, at 4.5, since it remained stable when stationary and responsive during motion.

C. Discussion

These results indicate that the prototype fulfils its intended role as a proof-of-concept rather than a finished product. The static tests in Fig. 7 and Fig. 8 confirm that the system reproduces both the direction and magnitude of roll and pitch compensation, with any small remaining deviation likely caused by sensor mounting or minor irregularities in the 3D-printed housing. The strong dynamic roll results demonstrate that the system responds correctly to motion as well as to a fixed position. The weaker dynamic pitch results suggest that the second axis functions in principle but is more sensitive to motion-related disturbances, in line with earlier findings from the software development stage.

The consistently high scores in Table II for rest stability, robustness, switch operation, brightness control, and repeatability are particularly relevant for a laboratory demonstrator because stable, predictable, and repeatable behaviour is more important at this stage than perfect performance in every individual motion test. The filter comparison provides the clearest technical justification for the selected design: the complementary filter offers the best balance between response speed and stability. For this reason, it was chosen as the practical default for the proof-of-concept system instead of the more advanced Madgwick filter.

VI. Conclusion

This paper presented a laboratory-based proof-of-concept for a low-cost, solid-state adaptive headlight control system that compensates for motorcycle pitch and roll. A prototype was built around an Arduino GIGA R1, a BMI270 inertial sensor, and WS2812-based NeoPixel LED rings, representing the beam through a symbolic, low-resolution cut-off model rather than a road-legal optical headlight. The system combined sensor acquisition, axis mapping, orientation estimation, and beam rendering, and compared accelerometer-only, Madgwick, and Complementary filtering to identify the most suitable approach for the demonstrator.

The completed system exhibited strong static roll and pitch behaviour, stable operation at rest, good repeatability, and a convincing dynamic response in roll. The dynamic pitch response remained less robust, confirming that the second axis is more sensitive to motion-related disturbances. However, the present work demonstrated that a solid-state adaptive headlight control concept can, in principle, be implemented for a motorcycle and can operate in a clear and repeatable manner under proof-of-concept conditions. This result should be considered alongside the main limitations of the work: the beam is a symbolic representation rather than a certified optical system; testing was carried out manually under simplified laboratory conditions rather than on a real vehicle; and dynamic pitch performance remains weaker than the roll.

References

[1] V. Cavallo, S. Espie, and N. Dang, "Improving motorcycle motion perception by using innovative motorcycle headlight configurations: Evidence from simulator and test-track experiments," *Accident Analysis and Prevention*, vol. 157, 2021, Art. no. 106118, doi: 10.1016/j.aap.2021.106118

[2] H. H. Vitca, I. A. Ştefan, and L. C. Miclea, "Computational procedure for adaptive front-lighting systems," in *Proc. 19th IEEE Int. Conf. on Intelligent Computer Communication and Processing (ICCP)*, Cluj-Napoca, Romania, 26-28 Oct. 2023, pp. 245–252, doi: 10.1109/ICCP60212.2023.10398728

[3] R. Radonjic, A. Jankovic, and B. Aleksandrovic, "The study of the single track vehicles dynamics," *Mobility and Vehicle Mechanics*, vol. 36, no. 3 pp. 23–33, Sep. 2010.

[4] S. Thomas, "Modelling and control of pitch-over phenomenon due to panic braking of motorcycles," MPil Thesis, Coventry Univ., Coventry, UK, 2014.

[5] A. Pena-Garcia, P. Pena, A. Espin, and F. Aznar, "Impact of adaptive front-lighting systems (AFS) on road safety: Evidences and open points," *Safety Science*, vol. 50, no. 4, pp. 945–949, 2012, doi: 10.1016/j.ssci.2011.10.013

[6] K. Rengade and V. K. Lamba, "Enhancing road safety through adaptive headlight system for two-wheelers," in *Proc. Intelligent Systems and Machine Learning Conf.*, Hyderabad, India, 4-5 May 2024, pp. 112–116, doi: 10.1109/ISML60050.2024.11007422

[7] S. P. K and G. S. S, "Adaptive headlamp design for two-wheelers: Enhancing nighttime visibility and safety,"in *Proc. Int. Symp. on Automotive Lighting* Darmstadt, Germany, 22–24 Sep. 2025, pp. 1–10.

[8] BMW Motorrad, "Adaptive headlight." [Online]. Available: https://www.bmw-motorrad.co.uk/en/engineering/detail/Safety/adaptive-xenon-headlight.html

[9] L. Nehaoua, H. Arioui, N. Seguy, and S. Mammar, "Dynamic modelling of a two-wheeled vehicle: Jourdain formalism," *Vehicle System Dynamics*, vol. 51, no. 5, pp. 648–670, 2013, doi: 10.1080/00423114.2012.762536

[10] R. Lot and J. Fleming, "Gyroscopic stabilisers for powered two-wheeled vehicles," *Vehicle System Dynamics*, vol. 57, no. 9, 2019, doi: 10.1080/00423114.2018.1506588

[11] R. Donadio, "Motorcycle cornering behaviour modelling," *Vehicle Technology Engineer*, vol. 1, no. 1, pp. 1–23, 2015, doi: 10.7790/vte-j.v1i1.8

[12] M. Bartolozzi, S. Bouaziz, G. Savino, S. Espie, "Data-driven methodology for the investigation of riding dynamics: A motorcycle case study," *IEEE Transactions on Intelligent Transportation Systems*, vol. 24, no. 9, pp. 10224–10237, 2023, doi: doi.org/10.1109/TITS.2023.3271790

[13] B. W. Weaver and P. R. DeLucia, "Effect of motorcycle lighting configurations on drivers' perceptions of closing during nighttime driving," *Transportation Research Part F: Traffic Psychology and Behaviour*, vol. 90, pp. 333–346, 2022, doi: 10.1016/j.trf.2022.08.017

[14] MR Presse, "Um die Kurve leuchten." [Online]. Available: https://www.motorradreporter.com/artikel/um-die-kurve-leuchten

[15] W. T. Neale, N. Mckelvey, D. Pentecost, and D. Koch, "Motorcycle headlamp distribution comparison," *SAE Technical Paper*, 2018-01-1037, 2018, doi: 10.4271/2018-01-1037

[16] H. V. Gautam *et al.*, "Evaluating the effect of oncoming vehicles glare on the visibility of behind-traffic sign boards," *SSRN Electronic Journal*, Apr. 2025, doi: 10.2139/ssrn.5222111

[17] J. Prasetijo *et al.*, "Visual performance and motorcycle safety-related impacts of various high beam headlight intensities," *Journal of the Society of Automotive Engineers Malaysia*, vol. 4, no. 1, pp. 35–43, 2020, doi: 10.56381/jsaem.v4i1.48

[18] N. Trivellin, M. Buffolo, C. De Santi, G. Meneghesso, E. Zanoni, and M. Meneghini, "Optoelectronic technologies for lighting in automotive: State-of-the-art and perspectives," in *Proc. AEIT Int. Conf. on Electrical and Electronic Technologies for Automotive*, Modena, Italy, 17-19 July 2023, pp. 1–6, doi: 10.23919/AEITAUTOMOTIVE58986.2023.10217200

[19] L. Zhang, M. Liu, Z. Sun, Y. Wu, and S. Zhou, "Requirements analysis and architecture design of automotive adaptive front-lighting system (AFS) based on functional safety standards," in *Proc. 22nd IEEE Int. Conf. on Industrial Informatics*, Beijing, China, 18-20 Aug. 2024, pp. 1–5, doi: 10.1109/INDIN58382.2024.10774379

[20] L. Lottner, M. Reiter, and B. Herrmann, "Automatic dynamic headlamp leveling utilizing camera-based vehicle pitch detection," in *Proc. Int. Symp. on Automotive Lighting* Darmstadt, Germany, 22–24 Sep. 2025, pp. 1–10, doi: 10.26083/tuprints-00030853

[21] T. A. Allsup, "Design and demonstration of an inertial-stabilized single-axis headlamp for mobile systems," PhD Thesis, Dept. of Mech. and Aerospace Eng., Univ. of Texas at Arlington, USA, 2023.

[22] J. K. Nkrumah, Y. Cai, and A. Jafaripournimchahi, “A review of automotive intelligent and adaptive headlight beams intensity control approaches,” *Advances in Mechanical Engineering*, vol. 16, no. 4, pp. 1–18, 2024, doi: 10.1177/16878132231220355

[23] B. Fal Desai, G. N. Deepak, C. H. Sanjay, Y. S. Nitin, S. Allurkar, “Adaptive matrix headlight control system in two-wheeler,” *International Journal of Advanced Research in Science, Communication and Technology*, vol. 5, no. 6, pp. 382–388, June 2025, doi: 10.48175/568

[24] I. A. Faisal, T. W. Purboyo, and A. S. R. Ansori, “A review of accelerometer sensor and gyroscope sensor in IMU sensors on motion capture,” *Journal of Engineering and Applied Sciences*, vol. 15, no. 3, pp. 826–829, 2019, doi: 10.36478/jeasci.2020.826.829

[25] D. Capriglione *et al.*, “Performance analysis of MEMS-based inertial measurement units in terrestrial vehicles,” *Measurement*, vol. 186, 2021, Art. no. 110237, doi: 10.1016/j.measurement.2021.110237

[26] H. Al Jlailaty, A. Celik, M. M. Mansour, A. M. Eltawil, “IMU hand calibration for low-cost MEMS inertial sensors,” *IIEEE Transactions on Instrumentation and Measurement*, vol. 72, 2023, Art. no. 7505516, doi: 10.1109/TIM.2023.3301860

[27] V. Suvorkin, M. Garcia-Fernandez, G. Gonzalez-Casado, M. Li, and A. Rovira-Garcia, “Assessment of noise of MEMS IMU sensors of different grades for GNSS/IMU navigation,” *Sensors*, vol. 24, no. 6, 2014, Art. no. 1953, 10.3390/s24061953

[28] D. Maceira, A. Luaces, U. Lugris, M. Á. Naya, and E. Sanjurjo, “Roll angle estimation of a motorcycle through inertial measurements,” *Sensors*, vol. 21, no. 19, 2021, Art. no. 6626, doi: 10.3390/s21196626

[29] P. Rzucidlo, G. Kopecki, P. Szczerba, and P. Szwed, “Analysis of stochastic properties of MEMS accelerometers and gyroscopes used in the miniature flight data recorder,” *Applied Sciences*, vol. 14, no. 3, 2024, Art. no. 1121, doi: 10.3390/app14031121

[30] K. Cocoli and L. Badia, “A comparative analysis of sensor fusion algorithms for miniature IMU measurements,” in *Proc. Int. Semin. on Intelligent Technology and Its Applications*, Surabaya, Indonesia, 26-27 Jul. 2023, pp. 239–244, doi: 10.1109/ISITIA59021.2023.10220994

[31] M. N. Oz, S. Budak, E. Kurnaz, and A. Durdu, “Orientation determination in IMU sensor with Complementary filter,” *Turkish Journal of Forecasting*, vol. 6, no. 1, pp. 34–39, 2022, doi: 10.34110/forecasting.1126184

[32] S. O. H. Madgwick, ”An efficient orientation filter for inertial and inertial/magnetic sensor arrays,” Dept. Mech. Eng., Univ. Bristol, Bristol, UK, Tech. Rep. 25, Apr. 2010.

[33] A. Juhas, “Control system for real-time interaction with LED matrix display,” BSc Thesis, Faculty of Informatics, Masaryk Univ., Brno, Czechia, 2025.